Received: 29 March 2017 | Revised: 21 October 2017 | Accepted: 27 December 2017

DOI: 10.1002/nag.2773

RESEARCH ARTICLE

WILEY

Explicit approximate analytical solutions of seepage-deformation in unsaturated soils

Jiwei Li | Changfu Wei

State Key Laboratory of Geomechanics and Geotechnical Engineering, Institute of Rock and Soil Mechanics, Chinese Academy of Sciences, Wuhan, Hubei 430071, PR China

Correspondence
Jiwei Li, State Key Laboratory of Geomechanics and Geotechnical Engineering, Institute of Rock and Soil Mechanics, Chinese Academy of Sciences, Wuhan, Hubei 430071, PR China.
Email: iamliji_007@126.com

Funding information
National Natural Science Foundation of China, Grant/Award Number: # 11372078, # 41272358, and #11502276

Summary

An approximate analytical solution is presented for the coupled seepage and deformation problem of unsaturated soils. Because of the matric suction dependence of both saturation and permeability coefficient, the coupled governing equations are strongly nonlinear. To obtain an analytical solution, these coupled governing equations are linearized and analytically solved for a specified saturation using the eigenfunction method. Then, the obtained analytical solutions are extended to the entire saturation range. Comparison between the current solution and the previous theoretical solution indicates that the proposed solution yields excellent results. Due to its analytical nature, the proposed procedure can be effectively used to obtain the solution of the coupled seepage and deformation of unsaturated soils.

KEYWORDS

analytical solution, coupled seepage and deformation, unsaturated soil

1 | INTRODUCTION

Many geotechnical problems, such as precipitation-induced slope failures and soil swelling and collapsing, involve the coupling of deformation and seepage in unsaturated soils. With their obvious robustness and accuracy, analytical solutions of such problems are helpful and sometimes even crucial in engineering practice. Because the conductivity and saturation of unsaturated soil are matric suction dependent, the governing equations for the coupled seepage and

Notation: a, air phase/ pore size distribution parameter; A_k, generalised Fourier coefficient for air; b, material constant; $\boldsymbol{b}$, body force per unit volume; B_k, generalised Fourier coefficient for water; C_{ai}, partial differential equation coefficient; C_{wi}, partial differential equation coefficient; $C_{vi}^{\ a}$, partial differential equation coefficient; $C_{vi}^{\ w}$, partial differential equation coefficients; $\boldsymbol{D}$, drained stiffness matrix of the soil; $f_1(z)$, initial pore-water pressure distribution; $f_2(z)$, initial pore-air pressure distribution; $\boldsymbol{F}$, ordinary differential equations initial conditions; $\boldsymbol{g}$, vector of gravitational acceleration; g, gravitational acceleration; h, soil depth; i, integer; j, integer; $\boldsymbol{k}$, intrinsic permeability of the soil; k, intrinsic permeability of the soil; k_{ai}, air permeability coefficient at i-th saturation interval; k_{ra}, relative air permeability; k_{rai}, relative air permeability at i-th saturation interval; k_{rw}, relative water permeability; k_{rwi}, relative water permeability at i-th saturation interval; k_{wi}, water permeability coefficient at i-th saturation interval; K_a, bulk modulus of air; K_s, bulk modulus of the solid grains; K_t, bulk modulus of the porous medium; K_{pi}, slope of the saturation to suction; $\boldsymbol{K}$, intrinsic permeability of the soil/ coefficient matrix; m, integer; n, porosity; $\boldsymbol{N}$, ordinary differential equations coefficient matrix; $\boldsymbol{p}$, pore pressure; p_a, pore-air pressure; p_{ai}, the i-th pore-air pressure component; p_c, matric suction; p_{ci}, matric suction at i-th saturation interval; p_w, pore-water pressure; p_{wi}, the i-th pore-water pressure component; p_0, air-entry value; $\boldsymbol{r}_i$, eigenvector (i, 1,2); s, solid phase; S, saturation; S_{arefi}, reference air saturation at i-th saturation interval; S_{refi}, reference saturation at i-th saturation interval; t, time; $\boldsymbol{u}$, displacement; u, displacement; u_i, the i-th displacement component; w, water phase; X, orthogonal function; z, vertical position coordinate; α, Biot coefficient; γ_a, air weight per unit mass; γ_w, water weight per unit mass; δ, Kronecker delta; $\boldsymbol{\varepsilon}$, soil skeleton strain; λ_i, eigenvalues of matrix (i, 1,2); μ_a, dynamic viscosity of air phase; μ_w, dynamic viscosity of water phase; ρ_a, intrinsic mass density of air phase; ρ_w, intrinsic mass density of water phase; $\boldsymbol{\sigma}$, total external stress; $\boldsymbol{\sigma}'$, effective stress; χ, effective stress parameter; ω_k, eigenvalues

deformation of unsaturated soils are strongly nonlinear. Thus, it is generally difficult to obtain an analytical solution for the problem. Perhaps because of this, most of the existing solutions of the coupled seepage and deformation problem are numerical.[1-5]

Compared with its numerical counterpart, an analytical solution, if available, is much more robust and straightforward, providing an exact solution of a set of fully coupled equations for the verification of computer codes and semi-analytical solutions. Thus far, several analytical and quasi-analytical solutions with different assumptions are available for the initial/boundary problems related to unsaturated soils. Without considering the coupling of seepage and deformation, Srivastava and Yeh[6] derived an analytical solution for 1-dimensional rainfall infiltration toward the water table through homogeneous and 2-layer soils. Zhan and Ng[7] used Srivastava and Yeh's solution to discuss the effect of hydraulic parameters and rainfall conditions on the infiltration of unsaturated ground. Raats and Gardner[8] introduced a method to linearize the Richards equation using the Kirchhoff's integral transformation. Basha[9] used the Green's function to derive multidimensional nonsteady solutions for domains with prescribed surface flux boundary conditions and bottom boundary conditions. Malekzadeh and Pak[10] presented an analytical solution to a 1-dimensional fully coupled problem, in which the coefficients of the system of equations were assumed to be constant for the entire domain.

Neglecting the effect of pore air, Wu and Zhang[11] derived an analytical solution to the coupled seepage and deformation of homogeneous unsaturated soils by virtue of the Fourier integral transformation. In this solution, the analytical solution was obtained for a constant boundary and a constant porosity. Using linear elastic constitutive relationship, Wang and Li[12] derived analytical solutions to the 1-dimensional coupled seepage and deformation equations of unsaturated soils with 3 typical nonhomogeneous boundary conditions.

In this study, the governing equations of fully coupled seepage and deformation for unsaturated soils are first derived. The coupled equations are then linearized, and the approximate analytical solution of the linearized coupled equations is obtained for arbitrary initial and boundary conditions. Examples with 2 typical boundary conditions are presented to illustrate the validity of the solution.

2 | GOVERNING EQUATIONS

2.1 | Balance equations

The unsaturated soils under consideration are viewed as the porous continua composed of a solid matrix (s) with interconnected pores saturated with water (w) and air (a). Each bulk phase is endowed with its own kinematics, mass, and momentum, occupying the entire volume of the unsaturated porous media, V. Without loss of generality, it is assumed hereinafter that (1) an isothermal condition prevails in the spatial domain of concern, (2) the deformation of the soil matrix is linear elastic and infinitesimal, (3) the pore water is incompressible, (4) the effects of hysteresis are ignored, and (5) the pore gas is an ideal gas. In addition, both the gas and water phases are viewed as simple fluids, ie, all the effects of species diffusion in either water or gas phase are excluded.

Under the above assumptions, the coupled differential equations governing the flow of water and air through an unsaturated porous medium can be written as[13]

$$n\frac{\partial S}{\partial t}+S\nabla\cdot\frac{\partial \mathbf{u}}{\partial t}=\nabla\cdot\frac{\mathbf{k}k_{rw}}{\mu_w}(\nabla p_w-\rho_w\mathbf{g}) \tag{1}$$

$$n\frac{\partial(1-S)}{\partial t}+n(1-S)\frac{1}{K_a}\frac{\partial p_a}{\partial t}+(1-S)\nabla\cdot\frac{\partial \mathbf{u}}{\partial t}=\nabla\cdot\frac{\mathbf{k}k_{ra}}{\mu_a}(\nabla p_a-\rho_a\mathbf{g}) \tag{2}$$

where n is the porosity, S the saturation, ρ_α the intrinsic mass density of $\alpha(=a,s,w)$phase, $\mathbf{k}$ the intrinsic permeability of the soil, $k_{r\alpha}$ the relative permeability with respect to the α phase, μ_α the dynamic viscosity of α phase, p_a the pore-air pressure, p_w the pore-water pressure, $\mathbf{g}$ the gravitational acceleration,$\mathbf{u}$ the displacement, and K_a the bulk modulus of air.

The linear momentum balance equation for the porous media as a whole is given by

$$\nabla\cdot\boldsymbol{\sigma}+\mathbf{b}=0 \tag{3}$$

where $\boldsymbol{\sigma}$ is the total external stress; $\mathbf{b}$ the body force per unit volume of the porous medium.

2.2 | Constitutive relationships

The constitutive equations complement the governing equations by providing additional relationships between the deformation and stress variables. To describe this relationship, the concept of effective stress is introduced. For unsaturated soils, the Bishop's effective stress[14] is adopted here, ie,

$$\boldsymbol{\sigma}' = \boldsymbol{\sigma} - p_a\boldsymbol{\delta} + \chi(p_a - p_w)\boldsymbol{\delta} \tag{4}$$

where $\boldsymbol{\sigma}'$ is the effective stress, χ is called the effective stress parameter or Bishop's parameter, ranging from 0 to 1 for dry and saturated conditions, respectively, and $\boldsymbol{\delta}$ is the Kronecker delta. The term $\boldsymbol{\sigma} - p_a\boldsymbol{\delta}$ in Equation 4 is commonly called the net stress, and $p_a - p_w$ represents the matric suction, also known as the capillary pressure.

A popular form of Equation 3 is achieved by assuming that the Bishop parameter χ is identical to the degree of saturation S,[15,16] ie,

$$\boldsymbol{\sigma}' = \boldsymbol{\sigma} - p_a\boldsymbol{\delta} + S(p_a - p_w)\boldsymbol{\delta} \tag{5}$$

To account for the compressibility of solid material, the so-called Biot coefficient can be introduced, and the effective stress equation then becomes

$$\boldsymbol{\sigma} = \boldsymbol{\sigma}' - \alpha(Sp_w + (1-S)p_a)\boldsymbol{\delta}. \tag{6}$$

The Biot coefficient, α, is given by $\alpha = 1 - K_t/K_s$, where K_t is the bulk modulus of the porous medium and K_s is the bulk modulus of the solid grains.

The stress-strain relationship can be expressed as

$$\boldsymbol{\sigma}' = \mathbf{D}:\boldsymbol{\varepsilon} \tag{7a}$$

where $\mathbf{D}$ is the drained stiffness matrix of the soil and $\boldsymbol{\varepsilon}$ is the soil skeleton strain.

Substituting Equation 7a into Equation 6, it can be obtained as

$$\boldsymbol{\sigma} = \mathbf{D}:\boldsymbol{\varepsilon} - \alpha(Sp_w + (1-S)p_a)\boldsymbol{\delta}. \tag{7b}$$

Assuming that the deformation of solid matrix is infinitesimal, the relationship between strain and displacement can be expressed as

$$\boldsymbol{\varepsilon} = \frac{1}{2}\left(\nabla\mathbf{u} + (\nabla\mathbf{u})^T\right). \tag{8a}$$

Taking Equation 8 into Equation 7b, it can be obtained

$$\boldsymbol{\sigma} = \mathbf{D}:\frac{1}{2}\left(\nabla\mathbf{u} + (\nabla\mathbf{u})^T\right) - \alpha(Sp_w + (1-S)p_a)\boldsymbol{\delta}. \tag{8b}$$

Substituting Equation 8b into Equation 3, the governing equation for the deformation model can be obtained as

$$\nabla\cdot\left(\mathbf{D}:\frac{1}{2}\left(\nabla\mathbf{u} + (\nabla\mathbf{u})^T\right) - \alpha(Sp_w + (1-S)p_a)\boldsymbol{\delta}\right) + \mathbf{b} = 0. \tag{9}$$

2.3 | Linearization of governing equations

Both the saturation and the permeability coefficient are functions of matric suction ($p_c = p_a - p_w$) in an unsaturated soil. Due to the presence of the saturation and permeability coefficient, the coupled differential equations are strongly nonlinear. This fact leads to difficulties in analytically solving the couple d governing equations. In order to obtain an analytical solution of the problem, it is instructive to linearize first the coupled governing equations. Supposed that the degree of saturation varies within a range from S_1 to S_2, ie, $S \in (S_1, S_2)$. To conduct the linearization, one may divide the interval $S \in (S_1, S_2)$ into m non-overlapping segments with uniform spacing, ie,

$$S_1 = S_{1_0} < S_{1_1} < S_{1_2} < \ldots\ldots < S_{1_m} = S_2 \tag{10}$$

$$S_{1_{i+1}} - S_{1_i} = \frac{S_2 - S_1}{m}, \quad i = 0, 1, 2, ..., m-1 \tag{11}$$

According to the principle of mathematical analysis, there exists an integer m such that

$$K_{p_i} = \frac{dS}{dp_{c_i}}, S_{1_i} \le S \le S_{1_{i+1}} \tag{12}$$

where K_{p_i} is constant. In addition, if $S_{1_i} \le S \le S_{1_{i+1}}$, the permeability coefficient can be assumed as a constant. Under these conditions, the linearization of the coupled governing equations can be obtained as

$$nK_{p_i}\left(\frac{\partial p_a - p_w}{\partial t}\right) + S_{ref_i}\nabla\cdot\frac{\partial \mathbf{u}}{\partial t} = \frac{\mathbf{k}k_{rw_i}}{\mu_w}\nabla\cdot(\nabla p_w - \rho_w \mathbf{g}) \tag{13}$$

$$-nK_{p_i}\left(\frac{\partial p_a - p_w)}{\partial t} + n\frac{S_{a_{ref_i}}}{K_a}\frac{\partial p_a}{\partial t} + S_{a_{ref_i}}\nabla\cdot\frac{\partial \mathbf{u}}{\partial t} = \frac{\mathbf{k}k_{ra_i}}{\mu_a}\nabla\cdot(\nabla p_a - \rho_a \mathbf{g}) \tag{14}$$

$$\nabla\cdot\left(\mathbf{D}\nabla\frac{\partial \mathbf{u}}{\partial t} - \alpha\left(S_{ref_i}\frac{\partial p_w}{\partial t} + S_{a_{ref_i}}\frac{\partial p_a}{\partial t}\right)\boldsymbol{\delta}\right) = 0 \tag{15}$$

where, $S_{ref_i} = (S_i + S_{i+1})/2$, and $S_{a_{ref_i}} = 1 - S_{ref_i}$.

For a 1-dimensional problem, the governing equations can be simplified as

$$nK_{p_i}\left(\frac{\partial p_a - p_w}{\partial t}\right) + S_{ref_i}\frac{\partial^2 u}{\partial z \partial t} = \frac{kk_{rw_i}}{\gamma_w \mu_w}\frac{\partial^2 p_w}{\partial z^2} \tag{16}$$

$$-nK_{p_i}\left(\frac{\partial p_a - p_w)}{\partial t} + n\frac{S_{a_{ref_i}}}{K_a}\frac{\partial p_a}{\partial t} + S_{a_{ref_i}}\frac{\partial^2 u}{\partial z \partial t} = \frac{kk_{ra_i}}{\gamma_a \mu_a}\frac{\partial^2 p_a}{\partial z^2} \tag{17}$$

$$D\frac{\partial^2 u}{\partial z \partial t} - \alpha\left(S_{ref_i}\frac{\partial p_w}{\partial t} + S_{a_{ref_i}}\frac{\partial p_a}{\partial t}\right) = 0. \tag{18}$$

Substituting Equations 18 into Equations 16 to 17, one obtains

$$\frac{\partial p_w}{\partial t} + C_{w_i}\frac{\partial p_a}{\partial t} = C_{v_i}^w\frac{\partial^2 p_w}{\partial z^2} \tag{19}$$

$$\frac{\partial p_a}{\partial t} + C_{a_i}\frac{\partial p_w}{\partial t} = C_{v_i}^a\frac{\partial^2 p_a}{\partial z^2} \tag{20}$$

which is subjected to the following initial conditions:

$$p_w(z, 0) = f_1(z), p_a(z, 0) = f_2(z) \tag{21}$$

where

$$C_{w_i} = \frac{nDK_{p_i} + \alpha S_{ref_i} S_{a_{ref_i}}}{\alpha S_{ref_i}^2 - nDK_{p_i}}$$

$$C_{v_i}^w = \frac{kk_{rw_i}D}{\alpha\mu_w\gamma_w S_{ref_i}^2 - \mu_w\gamma_w nDK_{p_i}}$$

$$C_{a_i} = \frac{nDK_aK_{p_i} + \alpha S_{ref_i} S_{a_{ref_i}} K_a}{nDS_{a_{ref_i}} + \alpha S^2_{a_{ref_i}} K_a - nDK_aK_{p_i}}$$

$$C^a_{v_i} = \frac{kk_{ra_i} DK_a}{\gamma_a \mu_a nDS_{a_{ref_i}} + \alpha \gamma_a \mu_a S^2_{a_{ref_i}} K_a - \gamma_a \mu_a nDK_aK_{p_i}}.$$

It should be noted that the governing equations, Equations 19 and 20, are a set of linear partial differential equations with constant coefficients in the saturation domain of $S_{1_i} \le S \le S_{1_{i+1}}$. This set of linear equations is fully coupled in nature. Compared with Equations 1 and 2, however, the difficulty in obtaining an analytic solution is greatly reduced. In the following, the analytical solution of the above linear system is obtained under some initial and boundary conditions. Then, an explicit approximate analytic solution of coupled problem in unsaturated soil is obtained by a continuation method.

3 | ANALYTICAL SOLUTION OF LINEARIZED GOVERNING EQUATIONS

Based on the eigenfunction method for linear partial differential equation and the principle of superposition,[17] the exact solutions for the governing equations, Equations 19 and 20 under a specific boundary condition, assume the following forms:

$$p_w = \sum_{k=0}^{\infty} A_k(t) X(\omega_k z) \tag{22}$$

$$p_a = \sum_{k=0}^{\infty} B_k(t) X(\omega_k z) \tag{23}$$

where $A_k(t)$ and $B_k(t)$ are generalized Fourier coefficients for air and water, respectively, both of which are functions of t. $X(\omega_k z)$ is a set of orthogonal functions determined from the boundary. The characteristic functions of different boundaries are shown in Table 1.

Substituting Equations 22 and 23 into Equations 19 to 21, and multiplying the resultants by $X(\omega_k z)$, and then integrating the resultants from 0 to h with respect to z, one obtains a family of ordinary differential equations as

$$\mathbf{N}\frac{d\mathbf{p}_k}{dt} = \mathbf{K}\mathbf{p}_k \tag{24}$$

$$\mathbf{p}_k(0) = \mathbf{F} \tag{25}$$

where,

$$\mathbf{p}_k = [A_k(t) \;\; B_k(t)]^T$$

TABLE 1 The characteristic functions of different boundaries

Boundary Condition at $z = 0$	Boundary Condition at $z = h$	$X(\omega_k z)$	Eigenvalues ω_k's are Positive Roots of	Description
$p_a = 0$	$\frac{\partial p_a}{\partial z} = 0$	$\sin(\omega_k z)$	$\cos(\omega_k h) = 0$	$\alpha = a$ or w
$\frac{\partial p_a}{\partial z} = 0$	$p_a = 0$	$\cos(\omega_k z)$	$\cos(\omega_k h) = 0$	
$p_a = 0$	$p_a = 0$	$\sin(\omega_k z)$	$\sin(\omega_k h) = 0$	
$\frac{\partial p_a}{\partial z} = 0$	$\frac{\partial p_a}{\partial z} = 0$	$\cos(\omega_k z)$	$\sin(\omega_k h) = 0$	

$$\mathbf{N} = \int_0^h X^2(\omega_k z)dz \begin{bmatrix} 1 & C_{w_i} \\ C_{a_i} & 1 \end{bmatrix}$$

$$\mathbf{K} = \int_0^h \frac{d^2X(\omega_k z)}{dz^2} X(\omega_k z)dz \begin{bmatrix} C_{v_i}^w & 0 \\ 0 & C_{v_i}^a \end{bmatrix}$$

$$\mathbf{F} = \frac{1}{\int_0^h X^2(\omega_k z)dz} \begin{bmatrix} \int_0^h f_1(z)X(\omega_k z)dz & \int_0^h f_2(z)X(\omega_k z)dz \end{bmatrix}^T$$

Equation 24 can be solved in a straightforward way, yielding

$$\mathbf{p}_k = c_1 e^{\lambda_1 t}\mathbf{r}_1 + c_2 e^{\lambda_2 t}\mathbf{r}_2 \tag{26}$$

where, λ_1 and λ_2 are eigenvalues of matrix $\mathbf{N}^{-1}\mathbf{K}$, $\mathbf{r}_1$ and $\mathbf{r}_2$ are the corresponding eigenvector. $\mathbf{c} = [\mathbf{r}_1 \quad \mathbf{r}_2]^{-1}\mathbf{F}$.

One obtains the exact solutions of the linearized coupled governing equations in as follows,

$$\mathbf{p} = \sum_{k=0}^{\infty} \left[c_1 e^{\lambda_1 t}\mathbf{r}_1 + c_2 e^{\lambda_2 t}\mathbf{r}_2\right] X(\omega_k z) \tag{27}$$

where,$\mathbf{p} = [p_w(z,t) \quad p_a(z,t)]^T$.

4 | APPROXIMATE ANALYTICAL SOLUTION IN THE UNSATURATED SOILS

Because the analytical solution is obtained for the linearized coupled equations, the previously described analytical solution is effective in the small vicinity of the specified saturation. In order to obtain the solution over the full range of saturation, the analytical solution needs to be extended. To this end, recall that the analytical solution is obtained over the subinterval of saturation, $S_{1_i} \le S \le S_{1_{i+1}}$, over which the slope of the saturation to suction $K_{p_i} = dS/dp_{c_i}$ and permeability coefficients $k_{w_i}$and k_{a_i} are assumed constant. These parameters can be easily determined using some empirical formula. Now, if the pore-gas pressure, the pore-water pressure, and displacement are, respectively, denoted by $p_{a_i}(z,t)$, $p_{w_i}(z,t)$, and $u_i(z,t)$ in $S_{1_i} \le S \le S_{1_{i+1}}$, the approximate analytical solution over the whole range of saturation ($S_1 < S < S_2$) can be obtained as

$$p_a(z,t) = \sum_i p_{a_i}(z,t), p_w(z,t) = \sum_i p_{w_i}(z,t), \quad u(z,t) = \sum_i u_i(z,t). \tag{28}$$

5 | EXAMPLES

5.1 | Example 1

To validate the previously derived analytical solutions, a typical example is computed using both the current solutions and those developed by others (eg, Shan et al[18]). It is worthy of notice that the first example computes the analytic solution of the linearized equation. This example has been used as a benchmark by many others such as Shan et al[18] and Qin et al.[19] The parameters used in the calculations are

$$C_w = -0.75, \quad C_a = -0.0775134, \quad C_v^w = 5\times10^{-18}\text{m}^2/\text{s}, \quad C_v^a = 6.45\times10^{-7} \ \text{m}^2/\text{s}$$

$$h = 10\text{m}, \ f_1(z) = 40\text{kPa} \ f_2(z) = 20\text{kPa}.$$

Two typical boundaries are chosen as following:

1. For the 1-end drainage condition, the upper boundary is considered to be permeable to both air and water phases. The lower boundary is impermeable to both air and water phases, ie,

$$p_w(0,t) = 0, p_a(0,t) = 0 \tag{29}$$

$$\frac{\partial p_w}{\partial z}|_{z=h} = 0, \frac{\partial p_a}{\partial z}|_{z=h} = 0. \tag{30}$$

2. For the 2-end drainage condition, the lower boundary is permeable to both air and water phases, ie,

$$p_w(0,t) = 0, p_a(0,t) = 0 \tag{31}$$

$$p_w(h,t) = 0, p_a(h,t) = 0. \tag{32}$$

The variations of pore-water and pore-air pressures with time and soil depth are presented in Figures 1 and 2 for the 1-end and 2-end drainage conditions, respectively. It can be seen that as time elapses, both p_w and p_a gradually dissipate and finally approach to a stable value. Comparison between Figures 1 and 2 shows that both the pore-water and pore-air pressure distributions are closely related to the boundary conditions.

Figures 3, 4 show the variations of pore-water and pore-air pressures with time at different depths (A–B) and with soil depth at different times (C–D). As expected, the dissipation of pore-air pressure is faster than the pore-water pressure at a given depth. The analytical results by Shan et al[18] are also shown in the figure for comparison. It is found that identical results are obtained from both analytical solutions, showing the validity of the current solution. Comparing Figures 3 and 4 shows that both water and air pressures dissipate faster under the 2-end drainage condition than under the 1-end drainage condition.

5.2 | Example 2

Example 1 is the analytic solution of the linearized unsaturated seepage deformation coupling equation in the vicinity of a specified saturation and does not take into account the changes of saturation and permeability coefficients with saturation. In this example, the same boundary conditions are used as in example 1. The initial condition is assumed to be $f_1(z) = -30$kPa and $f_2(z) = 0$kPa. The other parameters for water and air used in the seepage analysis are shown in Table 2. The soil type is classified as sandy soil. Figure 5A shows the soil-water characteristic curve at different pore size distribution parameters ($p_0 = 1.5$ kPa), and Figure 5B depicts the relative permeability-saturation relationships for water and air, which are described by van Genuchten's model[20] and Mualem's model,[21] respectively, ie,

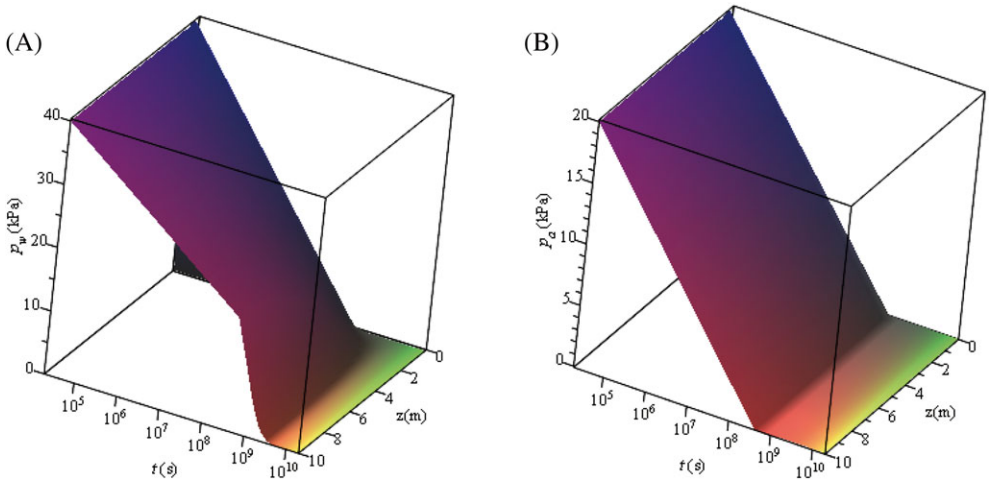

FIGURE 1 Variations of pore-water A, and pore-air B, pressures with time and soil depth for the 1-end drainage condition [Colour figure can be viewed at wileyonlinelibrary.com]

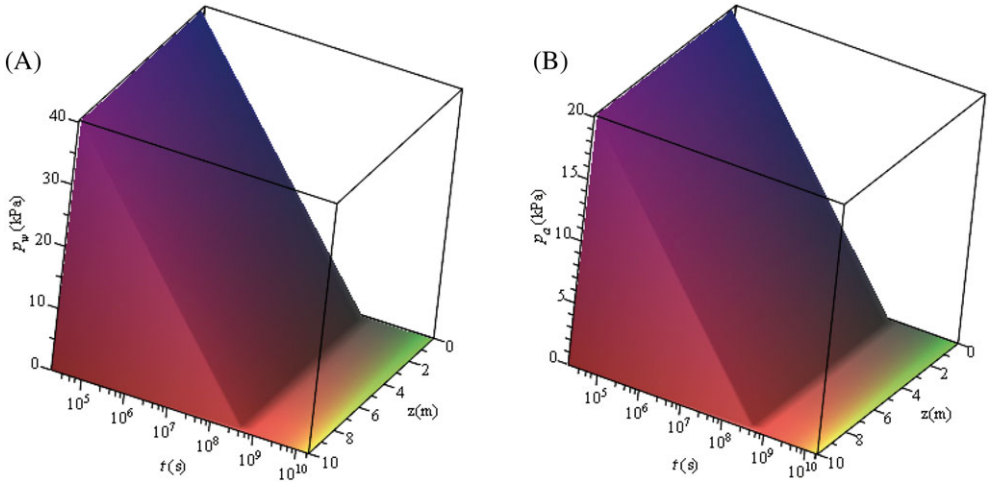

FIGURE 2 Variations of pore-water A, and pore-air B, pressures with time and soil depth for the 2-end drainage condition [Colour figure can be viewed at wileyonlinelibrary.com]

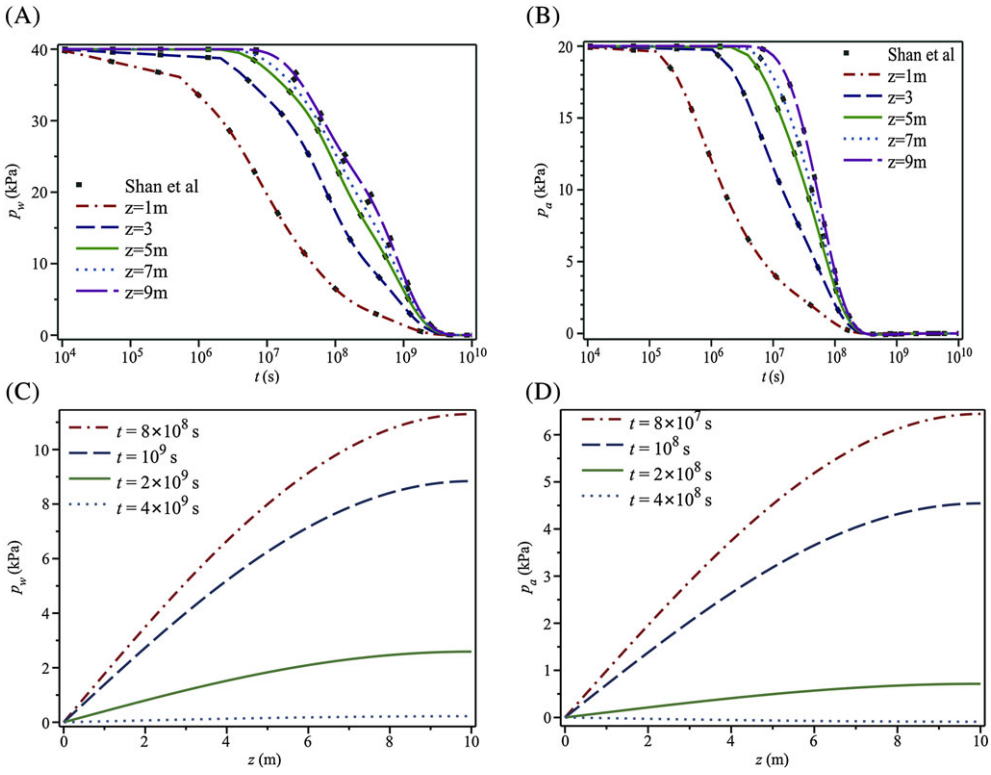

FIGURE 3 The variations of pore-water and pore-air pressures with time at different depths A-B, and with depth at different times C-D, for the 1-end drainage condition [Colour figure can be viewed at wileyonlinelibrary.com]

$$S = \left[1 + (p_c/p_0)^{\frac{1}{1-a}}\right]^{-a} \tag{33}$$

$$k_{rw} = S^b\left[1-\left(1-S^{1/a}\right)^a\right]^2 \tag{34}$$

$$k_{ra} = (1-S)^{1/2}\left(1-S^{1/a}\right)^{2a} \tag{35}$$

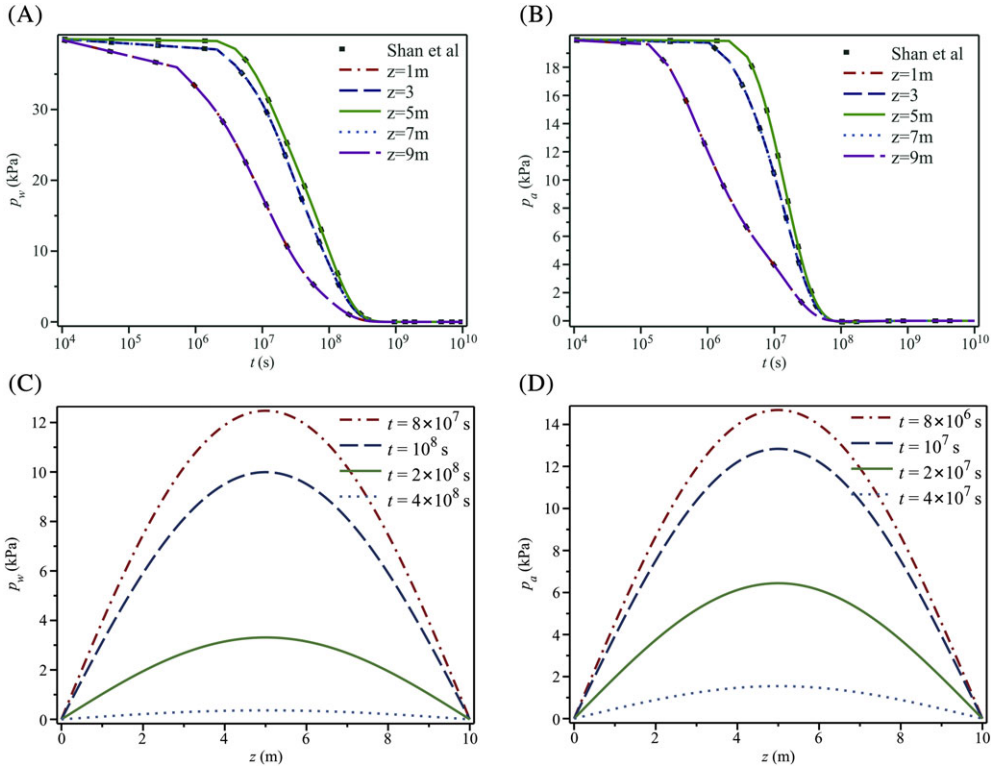

FIGURE 4 The variations of pore-water and pore-air pressures with time at different depths A-B, and with soil depth at different times C-D, for the 2-end drainage condition [Colour figure can be viewed at wileyonlinelibrary.com]

TABLE 2 Input parameters for analysis

Expression	Description	Parameter Value	Unit
Intrinsic permeability	k	10^{-13}	m^2
Air-entry value	P_0	1.5	kPa
Hydraulic constant	a	0.445	-
Hydraulic constant	b	0.5	-
Air dynamic viscosity	μ_a	0.018	g/m·s
Water dynamic viscosity	μ_w	1.0	g/m·s
Bulk modulus of water	K_w	2	GPa
Bulk modulus of air	K_a	0.1	MPa
Bulk modulus	K	33.3	MPa
Air density	ρ_a	1.25	kg/m^3
Water density	ρ_w	1000	kg/m^3
Porosity	n	0.35	-
Drained stiffness	D	11.1	MPa
Depth	h	10	m

where,p_0 is a parameter that depends approximately on the air-entry value, a is a parameter that is related to pore size distribution, and b is material constant.

Figures 6, 7 present the results of the 3-dimensional distribution of pore-water and pore-air pressures with time and soil depth for the 1-end drainage and the 2-end drainage conditions, respectively. It can be clearly seen that as time elapses, both p_w and p_a gradually dissipate and finally approach to a stable value. In addition, by comparing the results

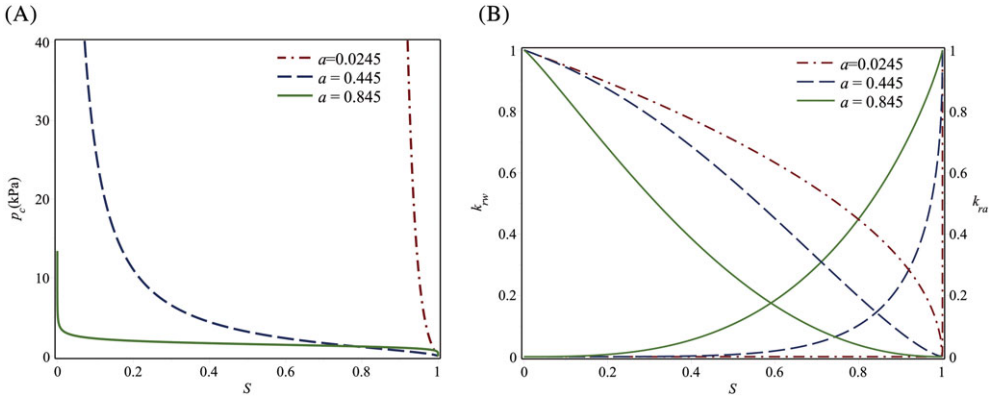

FIGURE 5 Hydraulic properties for seepage analysis. A, The degree of saturation vs capillary pressure curve at different pore size distribution parameters ($p_0 = 1.5$ kPa), and B, the relative permeability-saturation relationships for water and air at different pore size distribution parameters [Colour figure can be viewed at wileyonlinelibrary.com]

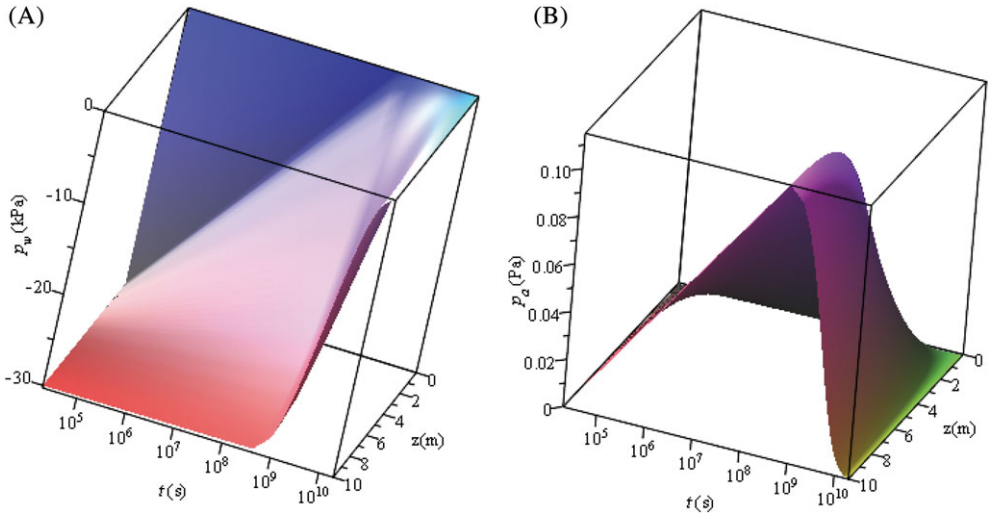

FIGURE 6 Variations of pore-water A, and pore-air B, pressures with time and soil depth for the 1-end drainage condition [Colour figure can be viewed at wileyonlinelibrary.com]

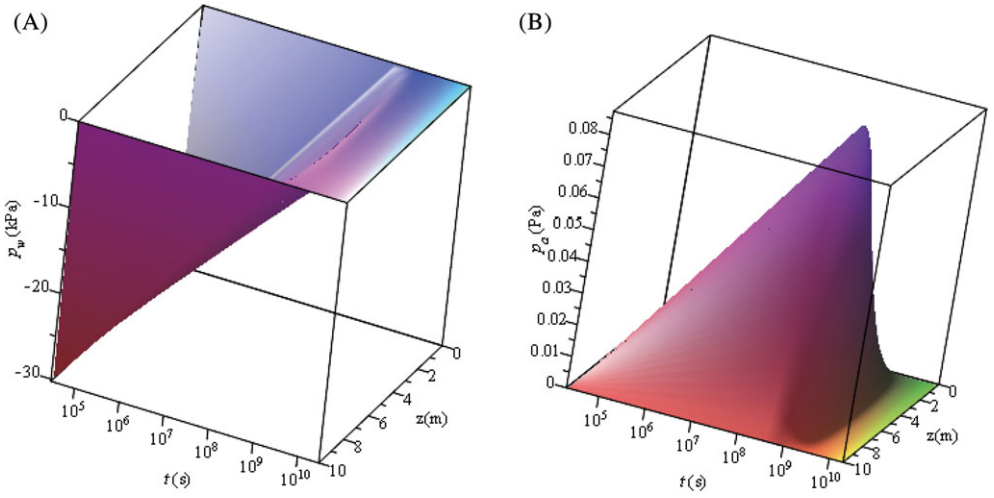

FIGURE 7 Variations of pore-water A, and pore-air B, pressures with time and soil depth for the 2-end drainage condition [Colour figure can be viewed at wileyonlinelibrary.com]

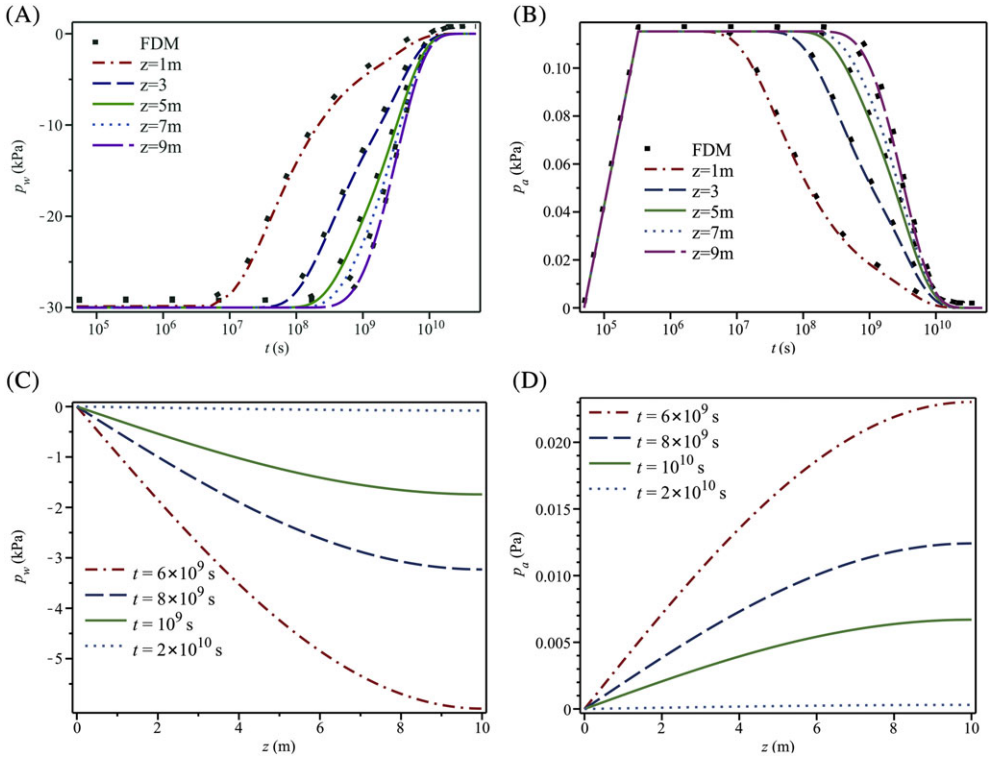

FIGURE 8 Variations of pore-water and pore-air pressures with time at different depths A-B, and with soil depth at different times C-D, for the 1-end drainage condition [Colour figure can be viewed at wileyonlinelibrary.com]

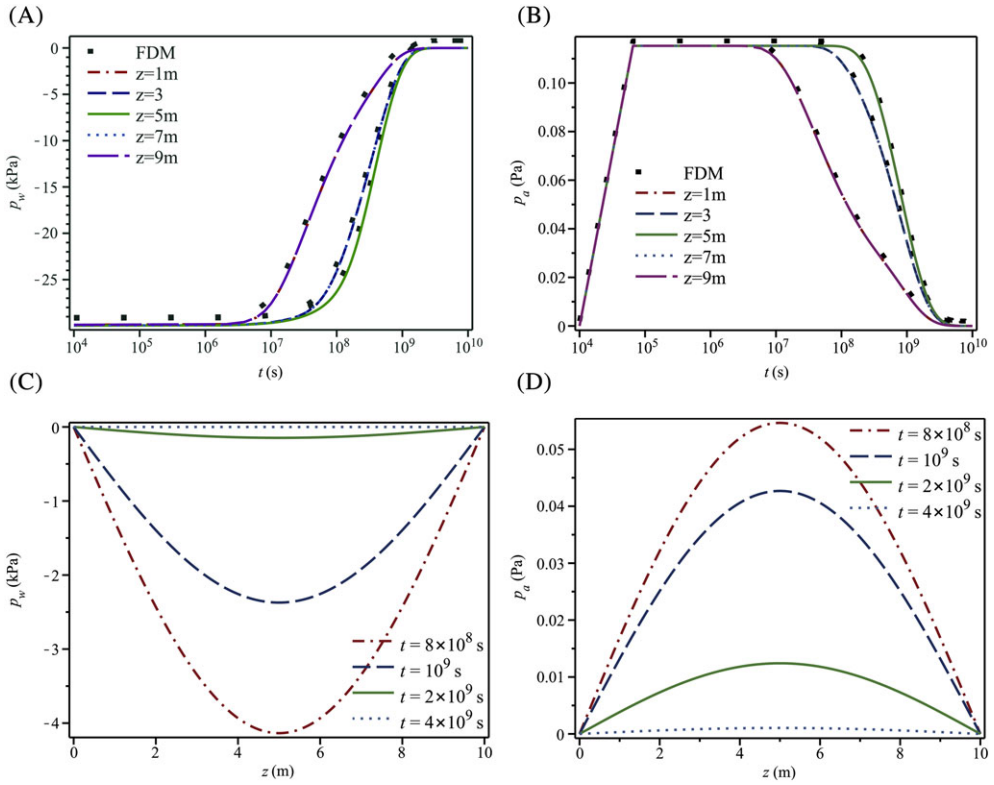

FIGURE 9 Variations of pore-water and pore-air pressures with time at different depths A-B, and with soil depth at different times C-D, for the 2-end drainage condition [Colour figure can be viewed at wileyonlinelibrary.com]

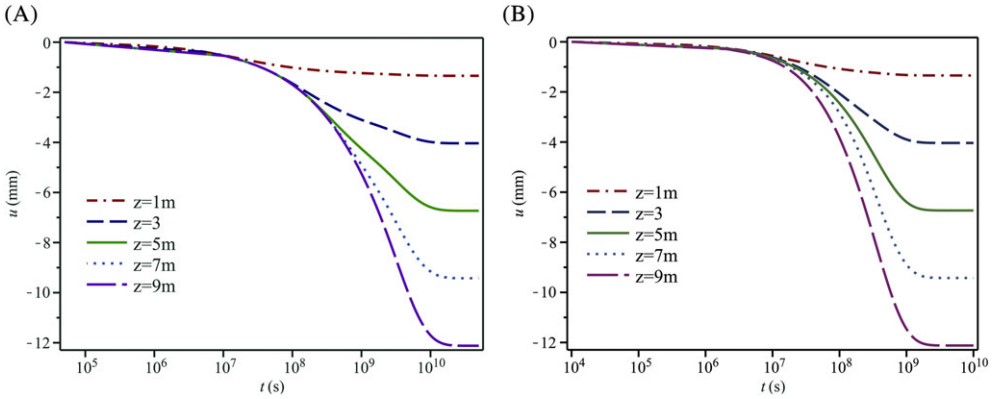

FIGURE 10 Variations of displacement with time at different depths for the 1-end drainage condition A, and the 2-end drainage condition B, [Colour figure can be viewed at wileyonlinelibrary.com]

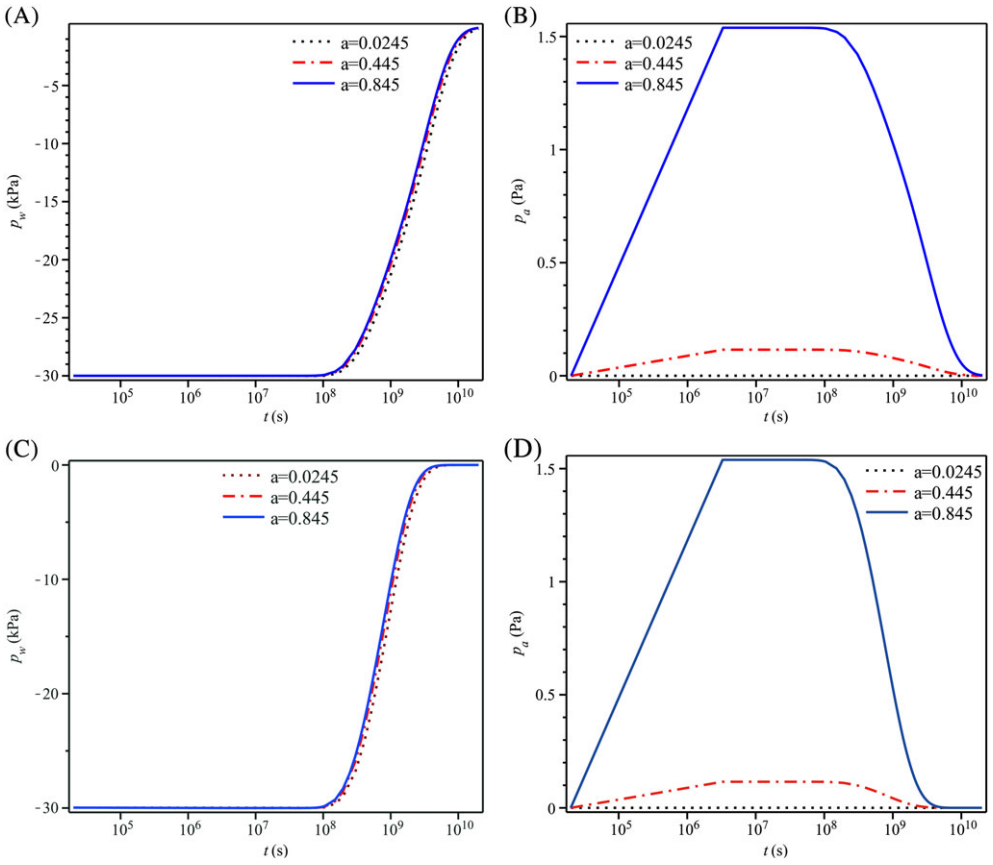

FIGURE 11 Variations of pore-water and pore-air pressures with time at different a for the 1-end drainage condition A-B, and the 2-end drainage condition C-D, (z = 5 m) [Colour figure can be viewed at wileyonlinelibrary.com]

in Figures 6 and 7, it can be observed that the boundary conditions have significant effect on the pore-water and pore-air pressures distribution.

Figures 8 and 9 depict the variations of pore-water, pore-air pressures with time at different depths and with soil depth at different times. It is shown that the dissipation of pore-air pressure is much faster than the pore-water pressure. In addition, although the fluctuation range of the pore-air pressure is very small, compared with the pore-water pressure, it is generally not negligible in the analysis of unsaturated problems (Sun et al, 2015[22]; Cho, 2016[23]). Figures 8 and 9 compare the results of the analytical solutions and the numerical results obtained by the finite difference method,[23,24] showing that the analytical solutions are consistent with the numerical results.

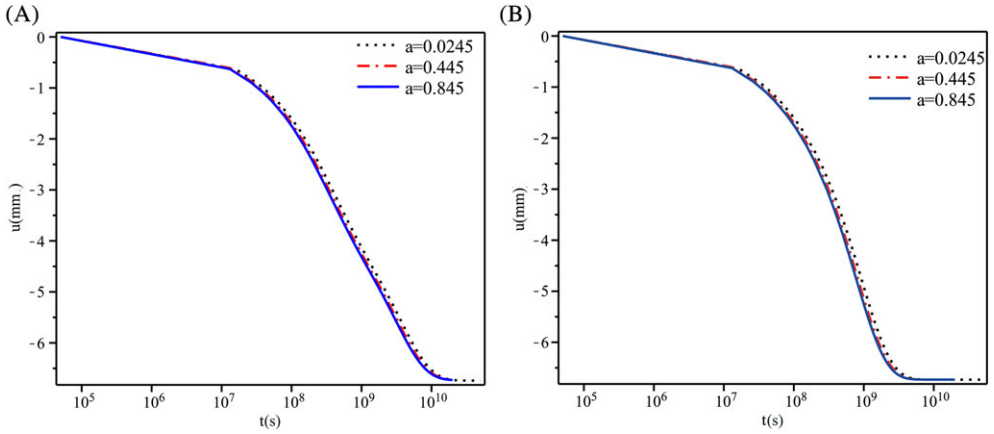

FIGURE 12 Variations of displacement with time at different a for the 1-end drainage condition A, and the 2-end drainage condition B, (z = 5 m) [Colour figure can be viewed at wileyonlinelibrary.com]

Figure 10 shows the variations of displacement with time at different depths for the 1-end drainage condition and the 2-end drainage condition. It can be observed that collapse is induced by the saturation process. The negative displacements gradually increase as time elapses and finally reach its maximum value. Moreover, the deeper the soil depth, the larger the amount of negative displacement. By comparing the results in Figure 10A,B, one can see that, as expected, the time for reaching the maximum negative displacement for the 2-end drainage condition is faster than the 1-end drainage condition.

Figures 11, 12 show the variations of pore-water and pore-air pressures and displacement with time at different a (z = 5 m). It reveals that as a increases, the pore pressure dissipates faster and negative displacement increases. That is, the more uniform the pore size distribution, the faster the pore pressure dissipates. In addition, the pore-air pressure increases more significantly with the change of parameter a compared with the pore-water pressure and displacement.

6 | CONCLUSION

In this study, an approximate analytical solution of 1-dimensional coupled seepage and deformation of unsaturated soils in any saturation interval is presented. The governing equations of coupled seepage and deformation are derived on the basis of mass conservation principle, Darcy law, and Bishop's effective stress model of unsaturated soils. Due to the presence of the saturation and permeability coefficient, the coupled differential equations are strongly nonlinear. After that, the linear coupled equation is obtained by linearizing the saturation and permeability functions. According to the characteristics of the linear equation and boundary conditions, the analytical solution is obtained by a linear superposition method. Finally, the analytical solution was further extended to the entire saturation interval. Excellent agreement has been found between the results obtained by the present solution and those derived from existing theoretical solutions.

In addition, based on the results of the approximate analytical solution, it can be found that effect of the change of boundary conditions on the change of the pore-air pressure and water pressure is significant. Although compared with the pore-water pressure, the fluctuation range of the pore-air pressure is very small, the dissipation of pore-air pressure is faster than the pore-water pressure. In addition, the more uniform the pore size distribution is, the faster the pore pressure dissipates.

ACKNOWLEDGEMENTS

This research was supported by the National Natural Science Foundation of China through Grants # 11372078, # 41272358, and #11502276.

ORCID

Jiwei Li http://orcid.org/0000-0002-5473-2165

REFERENCES

1. Sheng DC, Axelsson K. Uncoupling of coupled-flows in soil a finite-element method. *Int J Numer Anal Methods Geomech*. 1995;19(8):537-553.
2. Thomas HR, He Y. Analysis of coupled heat, moisture and air transfer in a deformable unsaturated soil. *Geotechnique*. 1995;45(4):677-689.
3. Schrefler BA, Xiaoyong Z. A fully coupled model for water flow and airflow in deformable porous media. *Water Resour Res*. 1993;29(1):155-156.
4. Kim JM. A fully coupled finite element analysis of water-table fluctuation and land deformation in partially saturated soils due to surface loading. *Int J Numer Methods Eng*. 2000;49(9):1101-1119.
5. Bandara S, Soga K. Coupling of soil deformation and pore fluid flow using material point method. *Comput Geotech*. 2015;63:199-214.
6. Srivastava R, Yeh TCJ. Analytical solutions for one-dimensional, transient infiltration toward the water table in homogeneous layered soils. *Water Resour Res*. 1991;27(5):753-762.
7. Zhan LT, Ng CWW. Analytical analysis of rainfall infiltration mechanism in unsaturated soils. *Int J Geomech (ASCE)*. 2004;4(4):273-284.
8. Raats PAC, Gardner WR. Movement of water in the unsaturated zone near a water table. In: van Schilfgraarde J, ed. *Drainage for Agriculture*. Madison, WI: Agronomy Monograph 17. American Society of Agronomy; 1974:311-357.
9. Basha HA. Multidimensional linearized nonsteady infiltration with prescribed boundary conditions at the soil surface. *Water Resour Res*. 1999;35(1):75-83.
10. Malekzadeh FA, Pak A. A discretized analytical solution for fully coupled non-linear simulation of heat and mass transfer in poroelastic unsaturated media. *Int J Numer Anal Methods Geomech*. 2009;33(13):1589-1611.
11. Wu LZ, Zhang LM. Analytical solution to 1D coupled water infiltration and deformation in unsaturated soils. *Int J Numer Anal Methods Geomech*. 2009;33(2009):773-790.
12. Wang H, Li J. Analytical solutions to the one-dimensional coupled seepage and deformation of unsaturated soils with arbitrary nohomogeneous boundary conditions. *Transp Porous Media*. 2015;108(2):481-496.
13. Muraleetharan KK, Wei C. Dynamic behaviour of unsaturated porous media: governing equations using the Theory of Mixtures with Interfaces (TMI). *Int J Numer Anal Methods Geomech*. 2015;23:1579-1608.
14. Bishop, AW. The principle of effective stress. Norges Getotekniske Institutt, 1960.
15. Lewis RW, Schrefler BA. The finite element method in static and dynamic deformation and consolidation of porous media. *Ann N Y Acad Sci*. 1998;366(1):62-74.
16. Gray WG, Schrefler BA. Analysis of the solid phase stress tensor in multiphase porous media. *Int J Numer Anal Methods Geomech*. 2007;31(4):541-581.
17. Pinchover Y, Rubinstein J. *An Introduction to Partial Differential Equations*. New York: Cambridge University Press; 2005.
18. Shan ZD, Ling DS, Ding HJ. Exact solutions for one-dimensional consolidation of single-layer unsaturated soil. *Int J Numer Anal Methods Geomech*. 2012;36(6):708-722.
19. Qin AF, Sun DA, Tan YW. Analytical solution to one-dimensional consolidation in unsaturated soils under loading varying exponentially with time. *Comput Geotech*. 2010;37(1-2):233-238.
20. van Genuchten MTA. Closed-form equation for predicting the hydraulic conductivity of unsaturated soils. *Soil Sci Soc Am J*. 1980;44(5):892-898.
21. Mualem Y. A new model for predicting the hydraulic conductivity of unsaturated porous media. *Water Resour Res*. 1976;12(3):513-522.
22. Sun DM, Zang YG, Semprich S. Effects of airflow induced by rainfall infiltration on unsaturated soil slope stability. *Transp Porous Media*. 2015;107(3):1-21.
23. Cho SE. Stability analysis of unsaturated soil slopes considering water-air flow caused by rainfall infiltration. *Eng Geol*. 2016;211:184-197.
24. Morton KW, Mayers DF. *Numerical Solution of Partial Differential Equations*. 2nd ed. Cambridge University Press; 2005.

How to cite this article: Li J, Wei C. Explicit approximate analytical solutions of seepage-deformation in unsaturated soils. *Int J Numer Anal Methods Geomech*. 2018;42:943–956. https://doi.org/10.1002/nag.2773